Detoxification of Chemical Warfare Agents by a Zr-Based MOF with High Recycling Ability at Physiological pH

Subharanjan Biswas, Rémy Gay, Janek Bzdrenga, Thomas Soirot, Nicolas Belverge, Nicolas Taudon, Xavier Brazzolotto, Mohamed Haouas, Nathalie Steunou, Jean-pierre Mahy, et al.

ACES Asian Chemical Editorial Society

doi.org/10.1002/cnma.202400132

CHEMNANOMAT
Research Article

www.chemnanomat.org

Detoxification of Chemical Warfare Agents by a Zr-Based MOF with High Recycling Ability at Physiological pH

Subharanjan Biswas[+],*[a] Rémy Gay[+],[a] Janek Bzdrenga,[b] Thomas Soirot,[b] Nicolas Belverge,[c] Nicolas Taudon,[c] Xavier Brazzolotto,[b] Mohamed Haouas,[d] Nathalie Steunou,[d] Jean-Pierre Mahy,[a] and Rémy Ricoux*[a]

The neutralization of organophosphorous (OP) chemical agents used in modern warfare is a growing concern due to their extreme toxicity to human cells. In several previous works, although the capability of several Zr-MOF-based catalysts has been showcased to facilitate hydrolysis of OP agents in heterogeneous pathways, their usage appeared to be limited by very slow kinetics at neutral pH. There is still a lack of MOF based catalysts that can detoxify OPs at physiological pH. The recycling ability of MOF-based catalysts has also not been greatly explored. Thus, herein, we explored a Zr-based MOF, MOF-801(Zr) for the detoxification of a series of OP nerve agents and a pesticide with simultaneous adsorption and degradation at pH 7.5 in a buffer solution, close to physiological conditions. This MOF-based catalyst demonstrates significant hydrolysis activity towards several nerve agents, with up to 99% conversion within 2 h and an excellent half-life of less than 5 minutes. In addition, it can be recycled at least 5 times consecutively with a residual activity of at least 90%.

Introduction

Chemical warfare agents (CWAs) are noxious chemicals designed to be used in warfare or closely associated military operations with the intent to harm, kill, or incapacitate adversaries.[1]

CWAs encompass various types, including nerve agents, blister agents (vesicants), blood agents, tear agents, and choking agents. Nerve agents are categorized as either G-type or V-type, stemming from alkyl phosphonate esters with different physicochemical properties.[1a–d] G-type nerve agents include compounds containing fluorine for sarin (GB), soman (GD), cyclosarin (GF) or cyanide for tabun (GA) as leaving groups (Figure 1). Such compounds are volatile and intoxication occurs mainly through the respiratory route.[2] On the contrary, V-type agents (such as VX) have thiol leaving groups and are more persistent, with a percutaneous intoxication route.[2]

Initial methods of detoxification of organophosphorus (OP) nerve agents include treating nerve agents-contaminated surfaces and equipment with strong alkaline solutions.[1b,3] This process leads to nucleophilic substitution of the leaving group at the phosphorus atom with hydroxyl, resulting in the formation of corresponding harmless phosphonic acids.[4] Albeit

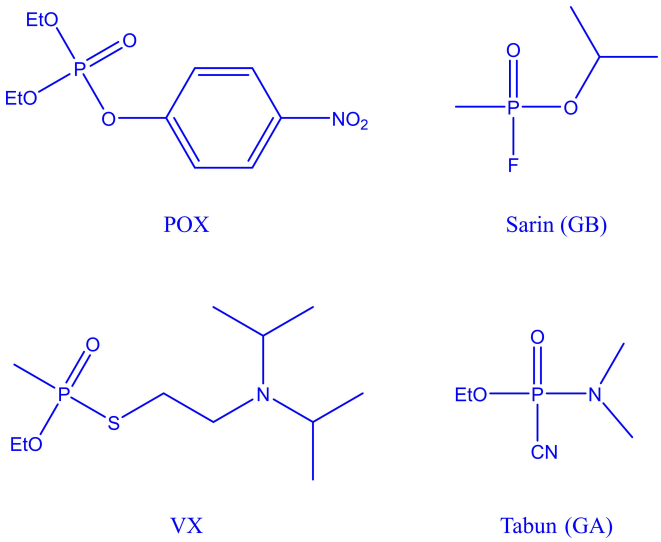

Figure 1. Organophosphates used for this study: Ethyl paraoxon (POX), Sarin (GB), VX and Tabun (GA).

[a] *Dr. S. Biswas,[+] R. Gay,[+] Prof. J.-P. Mahy, Dr. R. Ricoux*
Laboratoire de Chimie Bioorganique et Bioinorganique,
Institut de Chimie Moléculaire et des Matériaux d'Orsay,
UMR 8182, Bâtiment 670, Université Paris-Saclay,
17 Avenue des Sciences, 91400 Orsay, France
E-mail: remy.ricoux@universite-paris-saclay.fr
subharbiswas@gmail.com

[b] *Dr. J. Bzdrenga, T. Soirot, Dr. X. Brazzolotto*
Département de Toxicologie et Risques Chimiques
Institut de Recherche Biomédicale des Armées 1
Place du Général Valérie André, Brétigny-sur-Orge,
91220, France

[c] *N. Belverge, Dr. N. Taudon*
Analytical Developments and Bioanalysis Unit
Armed Forces Biomedical Research Institute
1 Place du Général Valérie André, Brétigny-sur-Orge,
91220, France

[d] *Dr. M. Haouas, Prof. N. Steunou*
Institut Lavoisier de Versailles, CNRS UMR 8180,
UVSQ Université Paris-Saclay,
78035 Versailles Cedex, France

[+] *These authors contributed equally.*

Supporting information for this article is available on the WWW under https://doi.org/10.1002/cnma.202400132

efficient, this approach has a few notable drawbacks. Firstly, it requires a significant surplus of base to ensure swift and thorough decontamination of the OP substrate. Secondly, the solution's highly alkaline properties pose risks of corrosion to various surfaces. Lastly, being a liquid-based decontamination approach, its integration into personal protection systems is challenging, thereby restricting its practical usage.[1a,5]

Hence, there is a pressing need for finding effective decontamination techniques capable of functioning under gentle conditions to bolster the mass elimination of nerve agent reserves and to create catalytic materials for immediate personnel safeguarding, including those seamlessly integrated into filters or interwoven into the textiles of personal protective equipment.[6] In response, researchers have explored various catalytic systems with the potential to meet these demands, with particular attention given to catalysts having metal oxides which have demonstrated considerable potential.[3,7]

Fundamentally, rapid catalytic hydrolysis of OP compounds at ambient conditions necessitates a couple of key elements: a Lewis acidic site to activate the phosphorus center, and a base to facilitate the availability of hydroxyl groups for the nucleophilic attack on the organophosphorus substrate. The blueprint for developing catalysts consisting of metal oxides for decontaminating OP nerve agents was initially influenced by biology, specifically enzymes such as phosphotriesterase characterized by bridged Zn(II) (Zn-OH–Zn), thus proficient in neutralizing OP compounds.[8] An obstacle to enzymatic hydrolysis of the nerve agents is a significant decline in enzyme activity at pH levels below 6.[9] Acidic by-products also emerge during the hydrolysis of some OP agents in acidic conditions.[9] This underscores the need for a class of durable and resilient materials capable of efficiently detoxifying OP agents. Drawing inspiration from the enzymes, scientists have delved into a relatively novel class of materials, metal organic frameworks (MOFs),[10] that possess the structural characteristics necessary for catalytic hydrolysis of OP agents, while also offering exceptional stability and permanent porosity as support.[7f,11]

MOFs represent a modern category of crystalline solids distinguished by their adjustable attributes like pore dimension, surface area and functionalities.[10,12] These frameworks are constructed through the creation of coordination bonds connecting metal-ion or metal-oxide clusters, clusters which are precursor of many functional materials,[13] often referred to as secondary building units (SBUs), with polytopic organic linkers. Utilizing the $Zr_6(\mu_3\text{-}O)_4(\mu_3\text{-}OH)_4$ SBU has enabled the synthesis of numerous MOFs capable of catalyzing the hydrolysis of OP agents, including highly hazardous CWAs. Due to their significant porosity and the robust Pearson hard-acid characteristics of their Zr(IV) sites, coupled with a strong affinity for phosphate compounds, Zr-based MOFs are being explored as highly promising materials for the safe disposal of OP pesticides and CWAs.[14] Moreover, the MOF nodes accommodating zirconium-bridging hydroxo ligands, bear a resemblance to the active sites of phosphotriesterase enzymes, containing bridged Zn(II) (Zn-OH–Zn). Analysis of available data has revealed various factors influencing degradation kinetics including strong Lewis acidity influencing activation of the P=O bond, while pore size facilitates access of the agent to the catalytic sites within the framework.[15]

Indeed, recent studies have demonstrated the effective hydrolysis of CWA agents or pesticides by some Zr-MOFs. Notably, a few investigations stand out, reporting the hydrolysis and capture of OP pollutants using Zr-MOFs such as NU-1000, PCN −777, MOF-808, UiO-66-NH_2, UiO-67 and their composites.[11a,14,16] Conversely, most of these Zr-MOFs exhibit hydrolytic degradation of organophosphorus compounds (OPs) in buffered media under significantly high alkaline pH conditions (pH 9–10), which, while being far from physiological conditions, also facilitates hydrolysis by itself. In miliQ water or in pH 7 solutions, conversion barely reaches 20–30 %[16a] with rare exceptions.[17] In addition, only few of those instances have been reported for the disposal of multiple pollutants, falling short of replicating real-world application conditions. [16a,17]

There is also a shortage of literature covering studies conducted at physiological pH. The degradation of CWAs in such conditions is imperative due to the potential threat these toxic substances pose to human health and safety. Replicating physiological pH to investigate OP hydrolysis not only closely mimics the conditions present within the human body but is also crucial for reducing corrosive damage initiated by high alkaline solutions and thereby simulating eco-friendly and biodegradable conditions. This approach should also be beneficial for devising countermeasures and treatments by facilitating a prompt response to chemical threats in emergency scenarios.

Recently, Some of us have reported a modified synthesis method for a well-known highly stable MOF, MOF-801(Zr), which shares a similar topology with UiO-66 (Figure 2a).[18] The ideal structure of MOF-801(Zr) involves the assembly of the $[Zr_6O_4(OH)_4]$ SBU with 12 ditopic fumarate linkers, resulting in a crystalline structure with a face-centered cubic topology.[18] By employing an excess amount of modulator, such as acetic acid, one not only can control the crystallization process to form uniform nanoparticles of the material but also introduce a large number of defects in the structure, leading to linker and/or metal vacancies. This, in turn, results in higher surface area, tunable porosity, and enhanced catalytic activity. In addition, the excellent water stability and the ideal pore structure for extensive ion conduction led us to explore this Zr-based MOF potential to hydrolyze OP toxic agents.

In this study, we demonstrate that MOF-801(Zr) can efficiently catalyze the hydrolysis of a series of OP pesticide and CWAs (viz., POX, GA, GB and VX, Figure 1) in close to physiological pH conditions, achieving conversion of up to 99 % of the OP agents with a maximum half-life of only 3.5 minutes.

Due to its heterogeneous nature and the ease of regenerating the catalyst, we have also demonstrated its recycling ability for at least 5 cycles with tremendous residual efficacy.

Results and Discussion

MOF-801(Zr) was synthesized according to a protocol previously reported by some of us[19] following an earlier study.[20] The

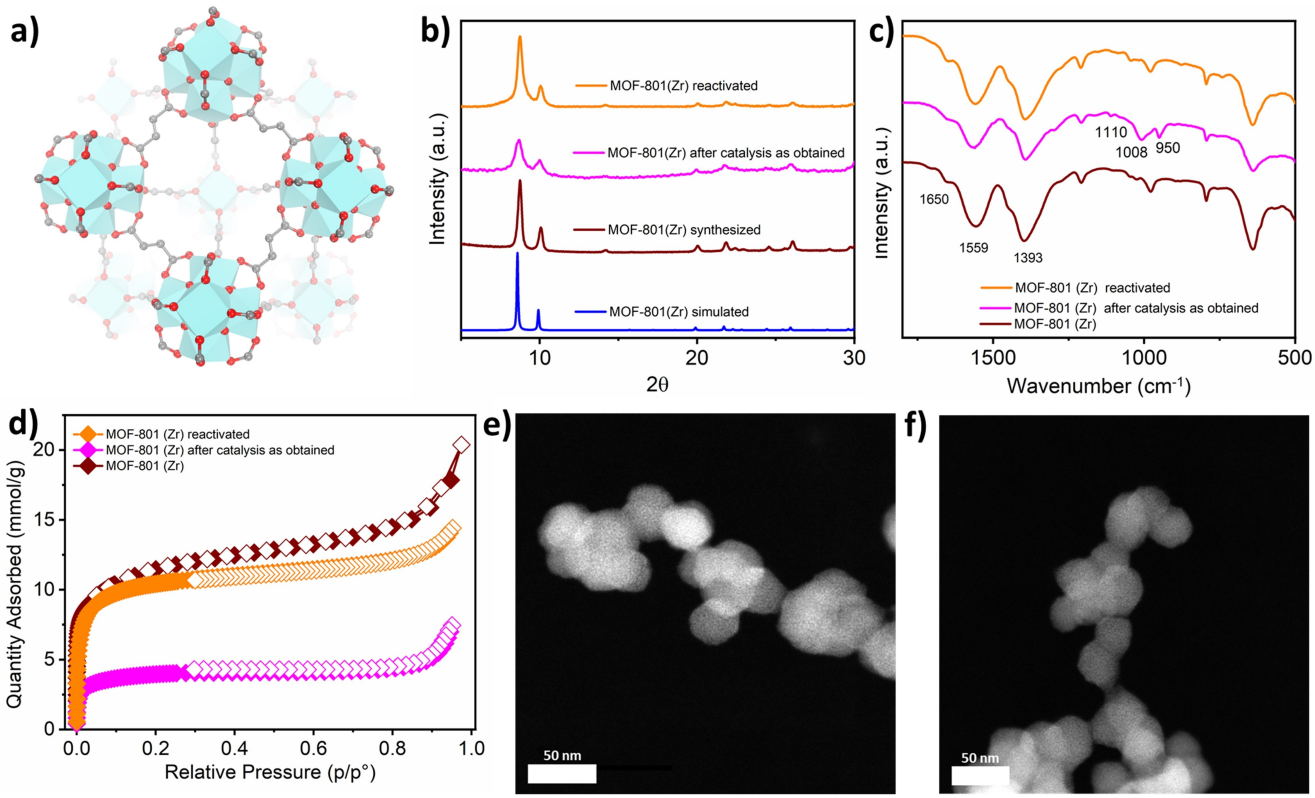

Figure 2. a) Structure of MOF-801(Zr). (b-d) Characterization of MOF-801(Zr), compared with as obtained MOF after catalysis and MOF after full recovery: b) Calculated and experimental PXRD patterns, c) FTIR spectra, d) N_2 adsorption – desorption isotherms (adsorption, filled symbols; desorption, empty symbols) at 77 K ($p° = 1$ atm). e) & f) HAADF-STEM images of pristine MOF-801(Zr).

PXRD pattern (Figure 2b) displays the characteristic Bragg peaks of the MOF-801(Zr) structure as shown previously and further physico-chemically characterized.[19] The FT-IR of MOF-801(Zr) (Figure 2c) displays characteristic vibration bands at 1393 and 1650 cm^{-1} corresponding to the -OCO- and C=O stretching modes respectively, a band at 1559 cm^{-1} for C=C stretching mode and at 793 cm^{-1} corresponding to the Zr–O stretching mode. MOF-801(Zr) was also characterized by N_2 porosimetry. It presents a type- I isotherm characteristic of a microporous material (Figure 2d). The Brunauer-Emmett-Teller (BET) surface area of 953 $m^2 g^{-1}$ is close to that previously reported for MOF-801(Zr) NPs.[19] As can be seen from HAADF-STEM images of the Figure 2e-f, MOF-801(Zr) consists of spheroidal nanocrystals with an average particle diameter of 30 nm and a quite narrow size distribution as previously reported.[19] Thermogravimetric analysis of the MOF allows to evaluate the ratio of the inorganic and organic part of the material suggesting 47% organic part and 53% inorganic part, very close to the calculated ratio obtained from molecular formula $\{Zr_6C_{24}H_{16}O_{32}\}$.[18] (Fig S1)

MOF-801(Zr) was synthesized using a high amount of modulator (acetic acid), which not only enables control over the crystallite size but also regulates the density of defects. Additionally, the inclusion of a modulator can significantly impact the porosity, hydrophilic–hydrophobic balance of the MOFs, and their adsorption or catalytic properties, as previously documented.[19][21] Defects occur when an organic linker (linker defects) or an entire zirconium cluster and its 12 associated linkers are absent (cluster defects), leading to the formation of mesopores and open coordination sites on SBUs crucial for high Lewis acidity.[21] We previously determined the composition and quantity of structural defects in this MOF using a combination of TGA, and ^1H and ^{13}C MAS NMR spectroscopy, as shown in table 1.[19] A significant amount of linker defects was found to be present in the MOF-801(Zr) since the connectivity of the $\{Zr_6\}$ oxo cluster was found to be close to 9, lower than that of 12 for a defect-free MOF-801(Zr).

Figure 3 shows the initial catalytic test towards the degradation of an OP pesticide, diethyl-4-nitrophenyl phosphate (POX,

Table 1. Structural properties and chemical composition of the MOF.[19] AcO and FA represent acetate and fumarate, respectively.

AcO/FA	Molecular formula	Defect level (%)	Connectivity of $\{Zr_6\}$ oxo cluster
0.62	$Zr_6O_{4.3}(OH)_{3.7}(FA)_{4.5}(AcO)_{2.7}$	25	9

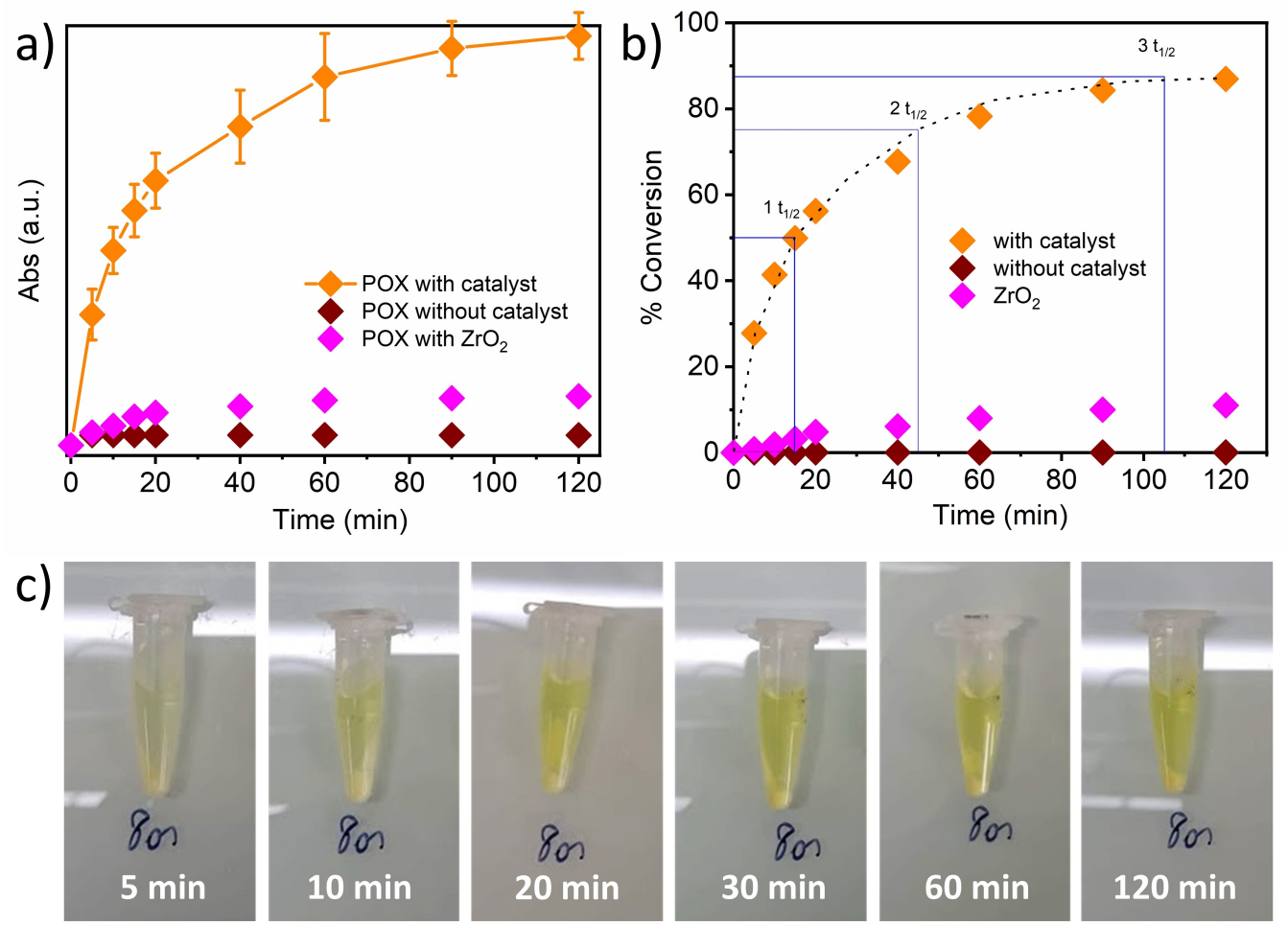

Figure 3. a) Evolution of the λ_{max} at 410 nm in UV-vis spectroscopy with course of the reaction of POX with MOF-801(Zr), in comparison with POX with no catalyst and ZrO_2 nanoparticles ($\Phi < 100$ nm). b) % conversion as calculated from ^{31}P NMR in course of the reaction. Dotted line indicates a 2nd order reaction pathway model. 1st, 2nd and 3rd $t^1/_2$ ($t^1/_2$, $t^3/_4$ and $t_{7/8}$ of the reaction are represented by blue vertical lines. c) Evolution of the intensity of the yellow coloration during the hydrolysis of POX, indicating the formation of 4-nitrophenoxide in solution.

3 mM), carried out using MOF-801(Zr) as catalyst (12 μmol) in 20 mM

TRIS buffer at pH 7.5 containing 0.15 M NaCl as reaction medium, to mimic a physiological medium. It is widely recognized that Zr-based MOFs or nanozymes facilitate the hydrolysis of hazardous OPs such as POX, leading to the generation of 4-nitrophenoxide and diethylphosphate (DEP).[22] As 4-nitrophenoxide exhibits a strong absorbance at 410 nm, it is thus convenient to monitor the progress of the hydrolysis reaction by following the increase of the intensity of its absorbance at this wavelength through UV-visible spectroscopy (Figure 3a). Figure 3a illustrates the initial 120-min segment of a representative absorbance evolution profile depicting the catalytic hydrolytic degradation of POX and its comparison with a blank control without catalyst and ZrO_2 nanoparticles. The percentage of conversion (Figure 3b) was calculated using ^{31}P NMR spectroscopy involving the comparison of integrations of an external standard (triethylphosphate, $\delta = 0$ ppm) with the ^{31}P chemical shift of POX ($\delta = -6.25$ ppm) and that of the hydrolysis product, DEP anion ($\delta = 1.5$ ppm) (Figure S2). Figure 3b shows that under the above-mentioned conditions a 50% conversion of POX was reached after a $t^1/_2$ value of 15 min. whereas 75% and 87.5% conversions were reached after the $t_{3/4}$ and $t_{7/8}$ values of about 30 and 60 minutes, respectively.

The conversion of POX reached a plateau value of ~89% after 2 h of reaction, most probably due to the saturation of the active catalytic sites with the hydrolyzed products leading to the deactivation of the catalytic centers. At any time point of the hydrolysis, extraction of the MOF by filtration from the reaction mixture caused an immediate termination of the reaction, demonstrating the role of MOF as a heterogeneous catalyst towards the hydrolytic degradation of POX (Figure S3).

Most of the studies on POX or DMNP hydrolysis report first-order or pseudo first-order kinetics studied at highly alkaline pH (~10).[16a] Generally the interaction of H_2O/OH^- with the OP substrate is defined as the rate limiting step of such reactions.[23] Thus, this is quite in line with the fact that at such pH values, there will be a large excess of hydroxyl ions, making the rate determining step to depend primarily on the activity of the substrate ($V = k_{app}[POX]$). In the case of a first-order reaction, one would expect a consistent value for successive half-lives. However, in the present case, as can be deducted from the

experimental rate plot in Figure 3b, the $t_{7/8}$ value (~60 min.) is about twice longer than the $t_{3/4}$ value (~30 min.) itself being about twice longer than the $t_{1/2}$ value (~15 min.), which is thus more consistent with a second order kinetics for the reaction. This is not surprising as in contrast to analogous reactions catalyzed at a higher pH (e.g., 10), in the current investigation, the solution pH (7.5) is only marginally alkaline, thereby minimizing the anticipation of a significant excess of the nucleophile OH^-. Instead, its participation in the rate-determining step alongside [POX] is consistent with a second order kinetics for the reaction with $v = k[OH^-][POX]$.

It is noteworthy that while the primary route for POX consumption is hydrolysis by the MOF, an important quantity of POX was also detected to be adsorbed within the porosity of the MOF, as evidenced by solid-state NMR spectroscopy on the MOF recovered after reaction (Figure S4). The ^{31}P NMR signal at −5.6 ppm indicates the presence of unreacted POX and the lack of the resonance of the hydrolyzed product at +2 ppm suggests its absence or presence in very few amounts.

It's important to mention that while the majority of the hydrolyzed product (DEP and 4-nitrophenoxide) was found in the solution, a small portion was also trapped within the MOF. This was indicated by the change in color of the recovered MOF, shifting from its original white color to yellow after the reaction (Figure 4b). Additionally, solid-state DRS (diffuse reflectance spectroscopy) reveals the emergence of a band at 375 nm throughout the reaction (Figure 4b). It is to be noted that although the λ_{max} of 4-nitrophenoxide in a solution with a pH of 7.5 is 410 nm, in solid-state DRS, the λ_{max} undergoes a blue shift to 387 nm, likely due to the absence of solvation (Figure 4a). Furthermore, a blue shift is also observed for 4-nitrophenoxide when encapsulated in the solid phase of MOF-801(Zr) to reach 379 nm, which could be attributed to the partial protonation of the phenolate groups by the H_2O groups present in the MOF (Figure 4a).

Following catalysis, the stability of the as obtained catalyst, without performing any activation protocol, was evaluated through a series of characterizations, including PXRD, FTIR, and N_2 porosimetry (Figure 2b-d). This as-obtained MOF-801(Zr) catalyst presumably contains a large number of trapped substrates and/or hydrolyzed product in the pores as shown by the decrease of the Bragg peaks intensity at low 2-theta angles {8.7 (111 plane) & 10 (200 plane)} in PXRD (Figure 2b), and the decrease of the surface area measured by N_2 porosimetry (Figure 2d) (449 m^2/g for the as-obtained MOF-801(Zr) after catalysis vs 953 m^2/g for the pristine MOF-801(Zr)). Furthermore, the FTIR spectrum (Figure 2c) of this material exhibited all the characteristic bands of MOF-801(Zr), with additional bands at 950, 1008, and 1110 cm^{-1}, which could be attributed to P-O symmetric stretch (950 cm^{-1}) and P–O asymmetric stretch (1008 cm^{-1} and 1110 cm^{-1}). This observation is expected to be due to the entrapment of both the substrate and the hydrolyzed DEP, which contain PO_4^{3-} groups.

Adsorption of the hydrolyzed product and unreacted substrate within the MOF was also found by solid-state DRS and solid-state NMR experiments (Figure 4 & S4), but the catalytic activity of MOF-801(Zr) could be recovered by washing thoroughly with water and subsequent drying in vacuum. Indeed, the characterization of the activated MOF-801(Zr) after catalysis by PXRD, FTIR and N_2 porosimetry indicates almost full recovery of the catalyst since its PXRD pattern, FT-IR spectrum and N_2 adsorption isotherm are comparable to that of the pristine MOF (Figure 2b-d).

All of these characterization data suggest recovery of the catalytic property of the material. Thus, the recycling ability of the MOF was worth being studied to assess the efficacy of MOF-801(Zr) for repetitive usage towards catalytic OP hydrolysis. A recyclability study using POX was conducted for 5 consecutive cycles of 1 h. As shown in Figure S5, the efficiency of the initial reaction with a pristine catalyst was considered to

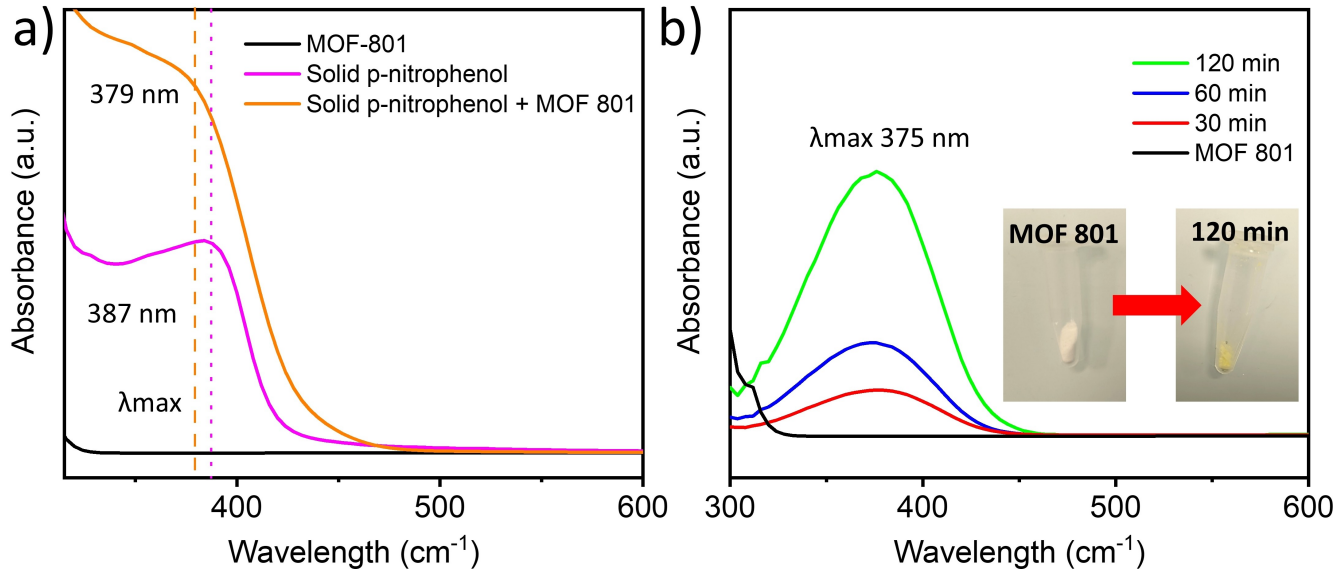

Figure 4. a) Solid state DRS (diffuse reflectance spectroscopy) of MOF-801(Zr), solid p-nitrophenol and p-nitrophenol in presence of MOF-801(Zr). b) Evolution of the λmax at 375 nm in solid state DRS UV-vis spectroscopy of the solid recovered after reaction with course of the reaction of POX with MOF-801(Zr).

be 100%. Upon recovering the catalyst and using it in additional cycles, the yield decreased slightly, fluctuating between 89% and 98% during the 5 cycles. These findings suggest a minimum degree of degradation of MOF over repetitive catalytic cycles.

Following the observation of highly promising catalytic activity with the OP pesticide POX, we next focused of the detoxification of real CWAs. Hydrolysis of GB and GA were followed by an enzymatic assay monitoring butyrylcholinesterase (BChE) inhibition[24] and that of VX by supercritical fluid chromatography (SFC, see experimental section for details). It is important to note that, due to the high toxicity of these compounds, using a high concentration such as that used previously for POX was not reasonable and lower toxic concentration had to be used. For BChE inhibition, 1.2 μmol of MOF 801(Zr) and desired concentration of one of the CWA agents were taken in TRIS buffer at pH 7.5 and incubated with BChE in phosphate buffer containing Ellman's reagent, 5,5′-dithiobis-(2-nitrobenzoic acid). The course of the reaction was monitored by measuring the absorbance of the 3-carboxy-4-nitrobenzenethiolate at 410 nm produced in the assay.

The hydrolysis rate of GB and GA with MOF at pH 7.5 proceeded with excellent $t_{1/2}$ of 4.5 and 3.5 minutes, respectively (Figure 5) in the tested conditions. Monitoring the hydrolysis of these CWA agents for 90 minutes showed that a very high conversions of 99% and 94% respectively could be achieved.

However, in the presence of the MOF, a slower hydrolysis of VX was observed in SFC, resulting in 69% conversion after 2 h of reaction with a $t_{1/2}$ value of 44 min, the slowest among all the 4 OPs (Figure 5), however over 98% conversion was detected after 4 h (Figure S6). Such slower kinetics could be attributed to the comparatively higher stability of the P-S bond compared to P–O or P-CN bonds, as well as higher hydrophobicity of VX compared to the other OPs. It is to be noted that SFC was performed in a non-targeted approach. After extraction of the ten most abundant peaks and structural identification using software, products resulting from the primary degradation pathways of VX, including cleavage of the P–S, S–C, and P–O bonds, were targeted. Unfortunately, none of these products were detected, particularly the highly toxic product EA2192.[25] The absence of detection of highly polar molecules could be explained by their trapping during the Solid-Liquid Extraction (SLE) step prior to SFC. An overlay of SFC chromatograms at different time points has been shown in the SI (Figure S7).

Table 2 presents a comparison between the current study and an earlier report regarding the hydrolysis of various OP agents by Zr-based MOFs at different pH values.[16a] For most OPs (such as POX, VX, and GA) at pH 10, several Zr-MOFs exhibited significant activity with faster kinetics, primarily attributed to the abundant presence of hydroxyl ions in the medium. However, the reaction notably decelerates at neutral pH, which is of course due to the decrease in the concentration in hydroxyl ions in medium that takes crucial part in both the catalysis as well as towards the regeneration of the catalyst. In our study conducted at pH 7.5, we observed significantly improved efficiency in most cases, with lower $t_{1/2}$ values than those reported in previous studies conducted at neutral pH.

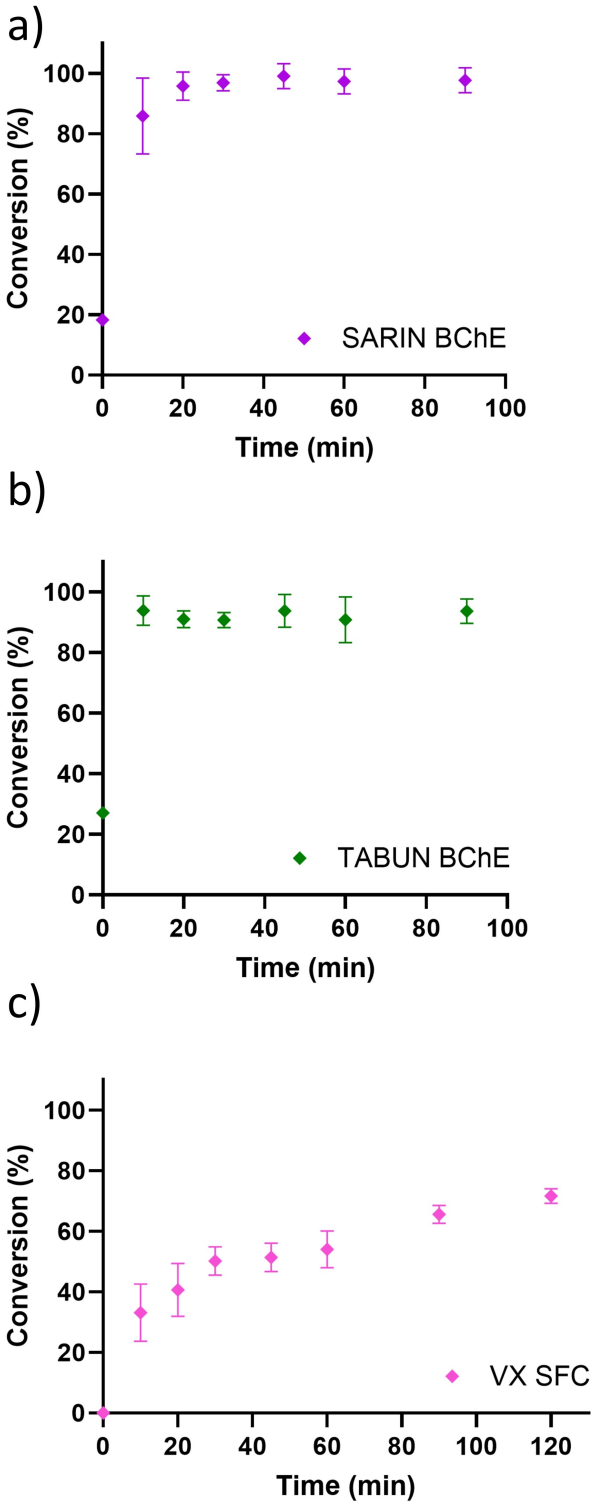

Figure 5. Conversion (%) towards the hydrolysis of CWAs by MOF-801(Zr): a) Sarin (GB) b) Tabun (GA) and c) VX.

Furthermore, the degradation of GB by Zr-based MOFs, which has been scarcely reported in the literature, occurred with an excellent conversion of 99% with an impressive $t_{1/2}$ of 4.5 min in our study. In the next section, a mechanism will be proposed to explain our results.

Table 2. Comparison among the efficiency of different Zr based MOFs towards OP hydrolysis reported earlier with reported in this study.

Subs.	MOF Catalyst	pH	$t_{1/2}$, min	Conv. (%)	Ref.
POX	NU-1000	10	2.6	100	[16a]
	MOF-808	10	3.6	100	[16a]
	UiO-66-NH_2	10	35	75	[16a]
	UiO-66-NH_2	7	99	21	[16a]
	MOF-801	7.5	15	89	This work
VX	NU-1000	10	5.3	100	[16a]
	MOF-808	10	<0.5	100	[16a]
	UiO-66-NH_2	10	2.2	100	[16a]
	UiO-66-NH_2	7	5	85	[16a]
	MOF-801	7.5	44	69	This work
GA	NU-1000	7	97	23	[16a]
	MOF-808	7	94	24	[16a]
	UiO-66-NH_2	7	39	33	[16a]
	MOF-801	7.5	3.5	94	This work
GB	MOF-801	7.5	4.5	99	This work

Efforts have been dedicated to comprehending the hydrolysis mechanism in these systems, utilizing both experimental and computational methodologies.[11c] Here, we propose a mechanistic pathway considering the previous literature and experimental evidences collected in this study (Figure 6). The degradation pathway involves hydrolysis followed by an adsorption step, wherein coordinated unsaturated Zr(IV) sites on MOF-801(Zr) coordinates with the P=O group of the OP agent (Figure 6a). Subsequently, a nucleophilic attack of a hydroxyl ion aided by a water molecule on the phosphorus atom leads to the removal of the leaving group (for example 4-nitrophenoxide in case of POX) from the OP after the formation of an intermediate. Eventually, the addition of water molecules liberates the Zr(IV) site, resulting in the formation of the less toxic phosphonate. In the case of POX hydrolysis, the ^{31}P NMR analysis confirmed the presence of DEP in the degradation of POX, while the evolution of the band at 410 nm with the progression of the reaction in UV-vis spectroscopy evidenced the production of 4-nitrophenoxide, in agreement with the proposed mechanism.

One of the most critical factors affecting the hydrolysis rate is the pH of the reaction medium. As the hydrolysis reaction

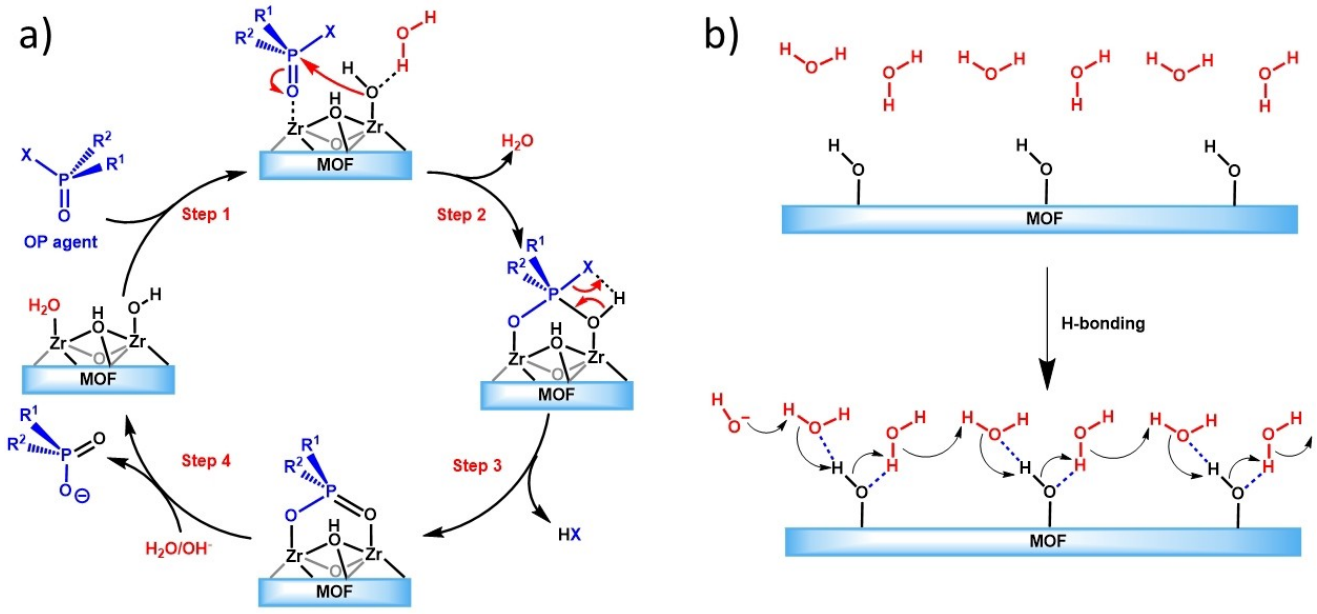

Figure 6. a) A proposed mechanism of hydrolysis of nerve agents by MOF-801(Zr), b) conduction of hydroxyl ions inside the cavity of the highly hydrophilic MOF-801(Zr), aided by μ_3-OH groups (only one connection shown for the sake of simple representation) facilitating hydrolysis of OP agents.

involves the nucleophilic attack of the organophosphorus compound by hydroxyl ligand aided by water molecule, reactions are typically conducted at alkaline pH values to ensure the presence of hydroxyl ions in large amount (usually pH ~9-10). In absence of base, on hydrolysis, the produced phosphonate also binds with the Zr_6 nodes very strongly, thus limiting further activity.[11c] Proton/hydroxyl ions are also believed to have an active part in the regeneration of the MOF after catalysis.

Thus, several studies conducted at pH 7 found a significant decrease in the rate constant and the conversion percentage. However, the present study conducted near physiological pH (7.5) shows a significant enhancement of both the rate and efficiency compared to reported studies at pH 7. This can be attributed to three principal reasons. Firstly, the slightly alkaline nature of the medium provides sufficient hydroxyl ions to take part in the reaction and for the regeneration of the catalyst. In addition, the structural features of MOF-801(Zr), including its inherent proton sources such as μ_3-OH groups, can promote the establishment of hydrogen bonding networks with water molecules in the surrounding environment,[26] thereby facilitating proton and hydroxyl ion transport (Figure 6b). Notably, as a result of the presence of fumaric acid, MOF-801(Zr) presents a high hydrophilic character and can adsorb a large amount of water in its tetrahedral and octahedral cavities that are prone to interact with the μ_3-OH groups of the framework through hydrogen bonds. Additionally, the intrinsic pore diameters of the structure range from 4.8 to 7.4 Å, resulting in narrow pore sizes that favor the organization of surrounding water molecules into an oriented hydrogen bonding system.[18a,26] These features of MOF-801(Zr) greatly enhance the ion conduction, thus facilitating the reaction at moderately alkaline pH (7.5). The importance of narrow pores, proton/hydroxyl conduction inside the MOF pore and the cooperativity among different catalytic sites was also evident by the fact that commercial ZrO_2 nanoparticles of diameter <100 nm only exhibited trace amount of hydrolysis in similar reaction conditions (Figure 3a-b).

Another significant factor that impacts the hydrolysis is the size of the MOF crystallites, where nanosized particles lead to faster substrate adsorption and product desorption owing to greater contact surface area with the substrate.[11c,27] Indeed, the crystallite size of MOF-801(Zr) synthesized in this study is close to 30 nm, which is significantly smaller than similar Zr based MOFs used in previous studies, thereby favoring the reaction at these conditions.

Conclusions

The rate and efficiency of the degradation of a chemically diverse range of organophosphate-based chemical warfare agents, including VX, GA, GB, and a pesticide, POX, were assessed in the presence of a Zr-based metal-organic framework MOF-801(Zr) which was used as a catalyst for the first time. The degradation rates were measured in a TRIS-buffer system of pH 7.5, to check the activity close to physiological conditions and to further elucidate the features and mechanisms governing these detoxification reactions. Experimental data revealed that the Zr-based MOF exhibited a significant potential for the decontamination of various OP agents under such conditions. It appeared that the potential of MOF-801(Zr) to form an extensive channel of water molecules aided by the μ_3-OH groups of the inner wall and favorable pore structure that influences extensive proton and hydroxyl conduction, finally led to the high efficiency of OP hydrolysis in a low alkaline medium. The nanometric size of MOF-801(Zr) crystallites, favored by the utilization of modulators during synthesis, also greatly influenced such high activity. Due to the heterogeneous nature of MOF and its easy recovery by simple filtration, it was possible to recycle it for at least 5 times without any significant loss of activity.

Experimental Section

Synthesis of MOF-801: The MOF was synthesized following the protocol we reported recently.[19]

POX hydrolysis: The UV-visible kinetics experiments were performed using centrifuged reaction mixture containing MOF-801(Zr), and POX TRIS buffer of pH 7.5 containing NaCl.

The reaction media after catalysis were further subjected to ^{31}P NMR analysis for the quantification of the product (DEP).

Recovery of catalyst and recycling tests: After each catalytic cycle the solid MOF was separated and reactivated before reuse.

Hydrolysis of CWAs

Caution! CWAs (GA, VX, GD) are extremely toxic compounds. Experiments involving these materials should only be conducted by trained personnel in a laboratory authorized to handle such materials.

BChE protocol: MOF-801(Zr) and Tabun or Sarin in TRIS buffer containing NaCl were added to BChE incubated in phosphate buffer to measure the according to Ellman's method by measuring the absorbance at 410 nm.

SFC: Reaction media of MOF-801(Zr) and VX in TRIS buffer containing NaCl were injected on SFC for analysis of hydrolysis.

More details about the experiments can be found in the SI.

Supporting Information

Additional experimental details, and additional characterization data are presented in the SI.

Acknowledgements

This work is part of the DetoxArtMet (ANR-21-CE390010) and Domino project (ANR-22-CE08-0007) funded by the National Research Agency. SB thanks Domino (ANR) for postdoctoral funding.

Conflict of Interests

The authors declare no conflict of interest.

Data Availability Statement

The data that support the findings of this study are available on request from the corresponding author. The data are not publicly available due to privacy or ethical restrictions.

Keywords: Chemical warfare agents · Pesticides · Organophosphate hydrolysis · Zr-based MOF · Detoxification

[1] a) B. Picard, I. Chataigner, J. Maddaluno, J. Legros, *Org. Biomol. Chem.* **2019**, *17*, 6528–6537; b) T. T. Marrs, R. L. Maynard, F. Sidell, *Chemical Warfare Agents: Toxicology and Treatment*, John Wiley & Sons, **2007**; c) S. S. Talmage, A. P. Watson, V. Hauschild, N. B. Munro, J. King, *Curr. Org. Chem.* **2007**, *11*, 285–298; d) E. J. Hulse, J. D. Haslam, S. R. Emmett, T. Woolley, *Br. J. Anaesth.* **2019**, *123*, 457–463; e) H. John, M. J. van der Schans, M. Koller, H. E. T. Spruit, F. Worek, H. Thiermann, D. Noort, *Forensic Toxicol.* **2018**, *36*, 61–71; f) O. I. Alsaleh, A. M. Elsafti El-saeidy, S. Saeed, A. Alhallak, M. A. Altelawi, G. Van Berlaer, I. Hubloue, *Cureus* **2022**, *14*, e22188; g) F. Moradi, M. Soderberg, F. Moradi, B. Daka, A. C. Olin, M. Larstad, *PLoS One* **2019**, *14*, e0218648.

[2] a) F. Nachon, X. Brazzolotto, M. Trovaslet, P. Masson, *Chem.-Biol. Interact.* **2013**, *206*, 536–544; b) G. Mercey, T. Verdelet, J. Renou, M. Kliachyna, R. Baati, F. Nachon, L. Jean, P. Y. Renard, *Acc. Chem. Res.* **2012**, *45*, 756–766; c) J. Bzdrenga, E. Trenet, F. Chantegreil, K. Bernal, F. Nachon, X. Brazzolotto, *Molecules* **2021**, *26*, 657; d) O. A. Lenina, I. V. Zueva, V. V. Zobov, V. E. Semenov, P. Masson, K. A. Petrov, *Sci. Rep.* **2020**, *10*, 16611.

[3] Y.-C. Yang, *Acc. Chem. Res.* **1999**, *32*, 109–115.

[4] G. W. Wagner, Y. C. Yang, *Ind. Eng. Chem. Res.* **2002**, *41*, 1925–1928.

[5] J. Nawała, P. Jóźwik, S. Popiel, *Int. J. Environ. Sci. Technol.* **2019**, *16*, 3899–3912.

[6] M. G. Holland, D. Cawthon, *Emerg. Med. Clin. North Am.* **2015**, *33*, 51–68.

[7] a) C. Bisio, F. Carniato, C. Palumbo, S. L. Safronyuk, M. F. Starodub, A. M. Katsev, L. Marchese, M. Guidotti, *Catal. Today* **2016**, *277*, 192–199; b) E. Denet, M. B. Espina-Benitez, I. Pitault, T. Pollet, D. Blaha, M. A. Bolzinger, V. Rodriguez-Nava, S. Briancon, *Int. J. Pharm.* **2020**, *583*, 119373; c) G. W. Wagner, in *Nanoscale Materials in Chemistry: Environmental Applications, Vol. 1045*, American Chemical Society, **2010**, pp. 125–136; d) P. Janos, J. Henych, O. Pelant, V. Pilarova, L. Vrtoch, M. Kormunda, K. Mazanec, V. Stengl, *J. Hazard. Mater.* **2016**, *304*, 259–268; e) I. Nath, J. Chakraborty, F. Verpoort, *Chem. Soc. Rev.* **2016**, *45*, 4127–4170; f) Y. Y. Liu, A. J. Howarth, N. A. Vermeulen, S. Y. Moon, J. T. Hupp, O. K. Farha, *Coord. Chem. Rev.* **2017**, *346*, 101–111; g) E. Barea, C. Montoro, J. A. Navarro, *Chem. Soc. Rev.* **2014**, *43*, 5419–5430; h) S. Kim, W. B. Ying, H. Jung, S. G. Ryu, B. Lee, K. J. Lee, *Chem. Asian J.* **2017**, *12*, 698–705; i) J. B. DeCoste, G. W. Peterson, *Chem. Rev.* **2014**, *114*, 5695–5727; j) N. S. Bobbitt, M. L. Mendonca, A. J. Howarth, T. Islamoglu, J. T. Hupp, O. K. Farha, R. Q. Snurr, *Chem. Soc. Rev.* **2017**, *46*, 3357–3385; k) S. Royuela, R. Gil-San Millan, M. J. Mancheno, M. M. Ramos, J. L. Segura, J. A. R. Navarro, F. Zamora, *Materials (Basel)* **2019**, *12*, 1974.

[8] a) K. Y. Wong, J. Gao, *Biochemistry* **2007**, *46*, 13352–13369; b) H. Carlsson, M. Haukka, E. Nordlander, *Inorg. Chem.* **2004**, *43*, 5681–5687; c) Z. Prokop, F. Oplustil, J. DeFrank, J. Damborsky, *Biotechnol. J.* **2006**, *1*, 1370–1380; d) A. N. Bigley, F. M. Raushel, *Biochim. Biophys. Acta* **2013**, *1834*, 443–453.

[9] B. M. Smith, *Chem. Soc. Rev.* **2008**, *37*, 470–478.

[10] a) H. Furukawa, K. E. Cordova, M. O'Keeffe, O. M. Yaghi, *The Chemistry and Applications of Metal-Organic Frameworks, Vol. 341*, **2013**; b) H. C. Zhou, S. Kitagawa, *Chem. Soc. Rev.* **2014**, *43*, 5415–5418; c) H. C. Zhou, J. R. Long, O. M. Yaghi, *Chem. Rev.* **2012**, *112*, 673–674; d) O. M. Yaghi, M. J. Kalmutzki, C. S. Diercks, *Introduction to Reticular Chemistry: Metal-Organic Frameworks and Covalent Organic Frameworks*, John Wiley & Sons, Germany, **2019**.

[11] a) M. J. Katz, S. Y. Moon, J. E. Mondloch, M. H. Beyzavi, C. J. Stephenson, J. T. Hupp, O. K. Farha, *Chem. Sci.* **2015**, *6*, 2286–2291; b) A. X. Lu, M. McEntee, M. A. Browe, M. G. Hall, J. B. DeCoste, G. W. Peterson, *ACS Appl. Mater. Interfaces* **2017**, *9*, 13632–13636; c) K. O. Kirlikovali, Z. Chen, T. Islamoglu, J. T. Hupp, O. K. Farha, *ACS Appl. Mater. Interfaces* **2020**, *12*, 14702–14720.

[12] a) A. Saad, S. Biswas, E. Gkaniatsou, C. Sicard, E. Dumas, N. Menguy, N. Steunou, *Chem. Mater.* **2021**, *33*, 5825–5849; b) S. Dasgupta, S. Biswas, K. Dedecker, E. Dumas, N. Menguy, B. Berini, B. Lavedrine, C. Serre, C. Boissiere, N. Steunou, *ACS Appl. Mater. Interfaces* **2023**, *15*, 6069–6078; c) E. Gkaniatsou, C. Sicard, R. Ricoux, L. Benahmed, F. Bourdreux, Q. Zhang, C. Serre, J. P. Mahy, N. Steunou, *Angew. Chem. Int. Ed.* **2018**, *57*, 16141–16146.

[13] a) S. Biswas, L. P. Datta, T. K. Das, *J. Mol. Eng. Mater.* **2022**, *10*, 2240004; b) S. Biswas, L. P. Datta, S. Roy, *J. Mol. Eng. Mater.* **2017**, *5*, 1750011; c) S. Biswas, L. P. Datta, T. K. Das, *New J. Chem.* **2022**, *46*, 7024–7031.

[14] L. González, R. Gil-San-Millán, J. A. R. Navarro, C. R. Maldonado, E. Barea, F. J. Carmona, *J. Mater. Chem. A* **2022**, *10*, 19606–19611.

[15] J. Tang, P. Li, T. Islamoglu, S. Li, X. Zhang, F. A. Son, Z. Chen, M. R. Mian, S.-J. Lee, J. Wu, O. K. Farha, *Cell Rep. Phys. Sci.* **2021**, *2*, 100612.

[16] a) M. C. de Koning, M. van Grol, T. Breijaert, *Inorg. Chem.* **2017**, *56*, 11804–11809; b) K. Ma, T. Islamoglu, Z. Chen, P. Li, M. C. Wasson, Y. Chen, Y. Wang, G. W. Peterson, J. H. Xin, O. K. Farha, *J. Am. Chem. Soc.* **2019**, *141*, 15626–15633; c) H. B. Luo, F. R. Lin, Z. Y. Liu, Y. R. Kong, K. B. Idrees, Y. Liu, Y. Zou, O. K. Farha, X. M. Ren, *ACS Appl. Mater. Interfaces* **2023**, *15*, 2933–2939; d) K. Kiaei, M. T. Nord, N. C. Chiu, K. C. Stylianou, *ACS Appl. Mater. Interfaces* **2022**, *14*, 19747–19755; e) J. Liu, H. Li, B. Yan, C. Zhong, Y. Zhao, X. Guo, J. Zhong, *ACS Appl. Mater. Interfaces* **2022**, *14*, 53421–53432.

[17] S. Y. Moon, G. W. Wagner, J. E. Mondloch, G. W. Peterson, J. B. DeCoste, J. T. Hupp, O. K. Farha, *Inorg. Chem.* **2015**, *54*, 10829–10833.

[18] a) H. Furukawa, F. Gandara, Y. B. Zhang, J. Jiang, W. L. Queen, M. R. Hudson, O. M. Yaghi, *J. Am. Chem. Soc.* **2014**, *136*, 4369–4381; b) G. Wißmann, A. Schaate, S. Lilienthal, I. Bremer, A. M. Schneider, P. Behrens, *Microporous Mesoporous Mater.* **2012**, *152*, 64–70.

[19] S. Biswas, M. Haouas, C. Freitas, C. Vieira Soares, A. Al Mohtar, A. Saad, H. Zhao, G. Mouchaham, C. Livage, F. Carn, N. Menguy, G. Maurin, M. L. Pinto, N. Steunou, *Chem. Mater.* **2022**, *34*, 9760–9774.

[20] M. R. DeStefano, T. Islamoglu, S. J. Garibay, J. T. Hupp, O. K. Farha, *Chem. Mater.* **2017**, *29*, 1357–1361.

[21] a) P. Iacomi, F. Formalik, J. Marreiros, J. Shang, J. Rogacka, A. Mohmeyer, P. Behrens, R. Ameloot, B. Kuchta, P. L. Llewellyn, *Chem. Mater.* **2019**, *31*, 8413–8423; b) G. C. Shearer, S. Chavan, S. Bordiga, S. Svelle, U. Olsbye, K. P. Lillerud, *Chem. Mater.* **2016**, *28*, 3749–3761; c) G. C. Shearer, J. G. Vitillo, S. Bordiga, S. Svelle, U. Olsbye, K. P. Lillerud, *Chem. Mater.* **2016**, *28*, 7190–7193; d) P. G. M. Mileo, K. H. Cho, J.-S. Chang, G. Maurin, *Dalton Trans.* **2021**, *50*, 1324–1333.

[22] K. Khulbe, G. Mugesh, *Polyhedron* **2019**, *172*, 198–204.

[23] E. Dyguda-Kazimierowicz, S. Roszak, W. A. Sokalski, *J. Phys. Chem. B* **2014**, *118*, 7277–7289.

[24] a) G. L. Ellman, K. D. Courtney, V. Andres, Jr., R. M. Feather-Stone, *Biochem. Pharmacol.* **1961**, *7*, 88–95; b) M. Trovaslet-Leroy, L. Musilova, F. Renault, X. Brazzolotto, J. Misik, L. Novotny, M. T. Froment, E. Gillon, M. Loiodice, L. Verdier, P. Masson, D. Rochu, D. Jun, F. Nachon, *Toxicol. Lett.* **2011**, *206*, 14–23.

[25] G. S. Groenewold, *Main Group Chem.* **2010**, *9*, 221–244.

[26] a) M. V. Nguyen, H. C. Dong, D. Nguyen-Manh, N. H. Vu, T. T. Trinh, T. B. Phan, *J. Sci. Adv. Mater. Devices* **2021**, *6*, 509–515; b) J. Zhang, H. J. Bai, Q. Ren, H. B. Luo, X. M. Ren, Z. F. Tian, S. Lu, *ACS Appl. Mater. Interfaces* **2018**, *10*, 28656–28663.

[27] K. Y. Cho, J. Y. Seo, H. J. Kim, S. J. Pai, X. H. Do, H. G. Yoon, S. S. Hwang, S. S. Han, K. Y. Baek, *Appl. Catal. B* **2019**, *245*, 635–647.

Manuscript received: February 28, 2024
Revised manuscript received: May 23, 2024
Accepted manuscript online: May 24, 2024
Version of record online: ■■, ■■

RESEARCH ARTICLE

Detoxification of organophosphate (OP) chemical warfare agents is a major concern due to their high toxicity. Previous researches demonstrate Zr-MOF catalysts efficiently hydrolyzing OPs in highly alkaline pH (~9-10). However, catalysts for detoxification at physiological pH and with high recycling ability remain limited. Here, we explore MOF-801(Zr) for OP detoxification at pH 7.5, showing significant catalytic activity, detoxifying up to 99% of pollutants within 2 h with fast $t_{1/2}$ of as low as 3.5 min, and retaining more than 90% of residual activity after 5 cycles.

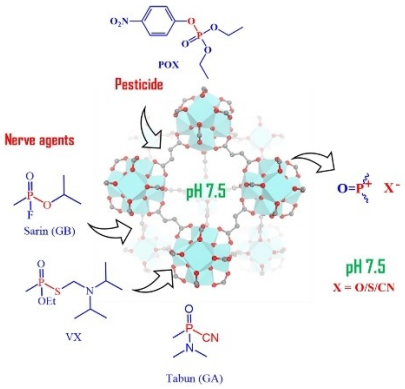

Dr. S. Biswas, R. Gay, Dr. J. Bzdrenga, T. Soirot, N. Belverge, Dr. N. Taudon, Dr. X. Brazzolotto, Dr. M. Haouas, Prof. N. Steunou, Prof. J.-P. Mahy, Dr. R. Ricoux**

1 – 10

Detoxification of Chemical Warfare Agents by a Zr-Based MOF with High Recycling Ability at Physiological pH